Cell, Vol. 91, 367–373, October 31, 1997, Copyright ©1997 by Cell Press

Cooking with Calcium: The Recipes for Composing Global Signals from Elementary Events

Martin D. Bootman*†, Michael J. Berridge,* and Peter Lipp*‡
*Laboratory of Molecular Signalling
The Babraham Institute, Babraham
Cambridge, CB2 4AT
United Kingdom
†Department of Zoology
University of Cambridge
Cambridge CB2 3EJ
United Kingdom

Summary

Recent studies have suggested that global intracellular Ca^{2+} signals arise from the summation and coordination of subcellular elementary release events (e.g., "Ca^{2+} puffs"), although the modes of recruitment of such signals are unknown. In order to understand how cells utilize elementary Ca^{2+} release events, we imaged Ca^{2+} transients evoked through the phosphoinositide pathway in HeLa cells using confocal microscopy. During the pacemaker phase leading to the global Ca^{2+} signal, elementary Ca^{2+} release events were recruited in (1) frequency, (2) amplitude, and (3) spatial domains. Since each digital elementary event contributes to a small change of the analog cytosolic Ca^{2+} concentration, the net effect of the advancement in the three domains is to drive the ambient Ca^{2+} concentration toward a threshold where the signal becomes regenerative, resulting in a global Ca^{2+} wave.

Introduction

Ca^{2+} is a ubiquitous intracellular signal, controlling diverse cellular functions (Berridge, 1993; Petersen et al., 1994; Clapham, 1995). In both excitable and nonexcitable cells, Ca^{2+} increases have a complex temporal and spatial arrangement (e.g., oscillations and waves) (Lechleiter et al., 1991; Thomas et al., 1991). Such global Ca^{2+} signals have been suggested to result from spatially and temporally coordinated recruitment of subcellular Ca^{2+} release units (Bootman and Berridge, 1995; Lipp and Niggli, 1996). These units represent the elementary building blocks of Ca^{2+} signaling, but the principles underlying their recruitment are largely unknown (Berridge, 1997). Examples of elementary Ca^{2+} release events are the "Ca^{2+} sparks" in cardiac muscle cells (Cheng et al., 1993; Lipp and Niggli, 1994; López-López et al., 1995) and the Ca^{2+} puffs in Xenopus oocytes (Yao et al., 1995), PC12 cells (Reber and Schindleholz, 1996), and HeLa cells (Bootman et al., 1997). Such elementary Ca^{2+} release events are short-duration, highly localized signals (Bootman and Berridge, 1995; Lipp and Niggli, 1996), which dissipate rapidly owing to diffusion in the cytoplasm and sequestration into the intracellular stores. Unless these Ca^{2+} release units become functionally coupled, such elementary releases always remain spatially restricted.

We previously observed that elementary signals such as Ca^{2+} puffs both initiated and propagated Ca^{2+} waves in hormonally stimulated HeLa cells (Bootman et al., 1997). Hormonal stimulation of cells effectively turns the cytoplasm into an excitable medium, since it evokes the production of the intracellular messenger inositol 1,4,5-trisphosphate ($InsP_3$), which diffuses into cells, binds to specific Ca^{2+}-releasing receptors ($InsP_3Rs$), and facilitates their activation by Ca^{2+} (Berridge, 1993; Petersen et al., 1994; Clapham, 1995). Ca^{2+} waves therefore reflect successive rounds of Ca^{2+} diffusion and Ca^{2+}-induced Ca^{2+} release (CICR) from $InsP_3Rs$. This saltatoric propagation of Ca^{2+} between functionally distinct elementary release sites underlies the regenerative spread of Ca^{2+} throughout the cells (Bootman et al., 1997). One key question concerning these processes is how the cell cytoplasm switches between localized elementary Ca^{2+} signals and regenerative global signals. Using confocal imaging of Fluo-3-loaded HeLa cells, we investigated the principal rules by which this transition is controlled.

Results and Discussion

Elementary Ca^{2+} Signals in Agonist-Stimulated HeLa Cells

HeLa cells displayed multiple levels of Ca^{2+} signaling in response to histamine stimulation: fundamental "Ca^{2+} blips" (Figure 1A) arising from the gating of single $InsP_3R$, intermediate Ca^{2+} puffs (Figure 1B) reflecting the coordinated recruitment of a cluster of $InsP_3Rs$, and propagating Ca^{2+} waves (Figure 1C). Ca^{2+} blips were distinguished from Ca^{2+} puffs by their kinetics and their amplitude. Ca^{2+} release events were referred to as blips (1) if they reached maximal amplitude within 130 ms and (2) when they had amplitudes of <40 nM. Ca^{2+} release events were regarded as Ca^{2+} puffs when (1) they reached their maximal amplitudes within 360 ms and when (2) their amplitude was ≥ 50 nM. Similar criteria were used to identify elementary events in Xenopus oocytes (Parker and Yao, 1996). Due to the acquisition rates of 7.5 or 15 Hz, the peaks of blips and puffs may be underestimated by a maximum of 25% (blip) or 10% (puff), as estimated by comparison with the kinetic data from a previous study (Bootman et al., 1997).

Since blips and puffs were sometimes observed during stimulation of an individual cell (data not shown) and could be evoked by the same histamine concentration (Figures 1A and 1B derived from different cells), these activities are not necessarily linked to actual $InsP_3$ concentrations. However, although different elementary Ca^{2+} signals can be evoked by a fixed histamine concentration (Figure 1A), increasing agonist concentrations enhanced the probability of a transition from nonregenerative Ca^{2+} release (Figure 2A) to regenerative Ca^{2+} waves (Figures 2B and 2C). Clearly, the crucial question is: what caused this transition?

‡To whom correspondence should be addressed.

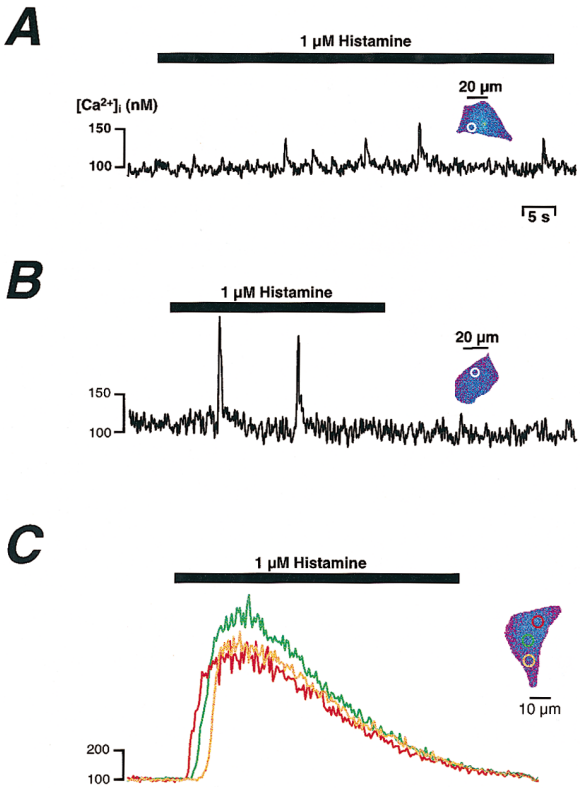

Figure 1. Elementary and Global Levels of Ca^{2+} Signaling in Agonist-Stimulated HeLa Cells

Application of an identical histamine concentration activates different subcellular patterns of Ca^{2+} release. (A) shows Ca^{2+} blips, resulting from the gating of a single (or a few) $InsP_3R$. Concerted activation of $InsP_3Rs$ produces the Ca^{2+} puffs shown in (B). Spatiotemporally coordinated recruitment of such elementary signals underlies propagating Ca^{2+} waves, as illustrated in (C). Note that the responses in (A–C) were acquired from different cells. The inset to each panel represents a confocal section through the cells at rest and depicts the location of the areas from which the $[Ca^{2+}]_i$ is plotted. For (C), the line plots indicate $[Ca^{2+}]_i$ in the localized regions shown in the inset with corresponding colors. The top bar in each panel marks the duration of histamine application. Note that all cells analyzed in this figure displayed only a single elementary Ca^{2+} release site.

One obvious change is that the frequency of the elementary events increased (Figure 2). Increases in frequency and closer functional coupling between release sites (Parker and Yao, 1991) are a consequence of the higher intracellular $InsP_3$ levels that occur with stronger stimulation of HeLa cells (Bootman et al., 1992) and serve to push the system over the threshold for global signals.

Recruitment in the Frequency and Amplitude Domains

The Ca^{2+} signals to very low and very strong stimulations represent the most intuitively understood patterns of response, since the former only evokes abortive, that is, nonregenerative, signals, whereas the latter always produces regenerative Ca^{2+} waves. However, the failure to become regenerative was not due to a lack of elementary Ca^{2+} release activity (e.g., Figures 2A and 3A). Instead, such failures reflect the inability of cells to reach a threshold for global Ca^{2+} waves.

Regenerative responses are usually preceded by a "pacemaker phase" during which elementary events increased in either frequency (Figure 3B) or amplitude (Figure 4). The cell response shown in Figure 3Ba, for example, displayed an increasing frequency of elementary events prior to the onset of regenerativity, while their amplitude remained constant (Figures 3Bb and 3Bc). Interestingly, the frequency and amplitude of the elementary signals in this cell were initially similar to the abortive cell in Figure 3A. However, whereas the latter displayed a slightly declining frequency, the increasing frequency in the regenerative cell enabled it to reach the threshold for global Ca^{2+} signals (Figure 3Bc).

The alternative behavior of elementary Ca^{2+} release events during the pacemaker is illustrated in Figure 4. In this cell, the frequency of elementary signals remained constant but their amplitude increased nearly 9-fold (from ~20 nM up to ~180 nM; Figures 4A, 4B, and 4D). Although the spatial spreading and amplitude of the signals increased, each elementary signal arose from the same subcellular locus (Figures 4E and 4G). The spatial properties of the elementary signals were assessed by fitting Gaussian distributions to the signals at their peak amplitudes (Figure 4F). Normalizing and superimposing the Gaussian curves revealed that the increased lateral spreading and amplitude of the Ca^{2+} release signals were due to an increased Ca^{2+} release flux from a point source, and not spatial recruitment of neighbouring Ca^{2+} release sites. Therefore, the growth of puff amplitudes described in Figure 4 was due to summation of coincident Ca^{2+} release from $InsP_3Rs$ within a cluster; a limited number of $InsP_3Rs$ contributed to the first release event, but activation of a successively increasing number of $InsP_3Rs$ caused the Ca^{2+} signal to increase.

The growth of pacemaker events such as those shown in Figure 4 has significant implications for our understanding of the functional structure of elementary Ca^{2+} release units. From the nature of the elementary events previously observed, a two-tier elementary Ca^{2+} signaling hierarchy was suggested (Bootman, 1996; Lipp and Niggli, 1996; Bootman et al., 1997; Lipp and Bootman, 1997). However, the present observation of elementary signals with variable amplitudes originating from a common point source contradicts the notion of stereotypic Ca^{2+} puffs. Instead, it appears that a variable number of $InsP_3Rs$ can be recruited from a cluster of $InsP_3Rs$, thus revealing a continuum of elementary Ca^{2+} signaling events. Within such a continuum, there is a minimal and a maximal boundary, represented at one extreme by the gating of single $InsP_3Rs$ (blips) and on the other by the concerted activation of an entire cluster. Consequently, blips are the exclusive unitary Ca^{2+} signaling events and represent the fundamental quantum of releasable Ca^{2+}. Ca^{2+} puffs are not stereotypic Ca^{2+} release events but reflect signals evoked by Ca^{2+} release from two $InsP_3Rs$ up to an entire $InsP_3R$ cluster. Although these data suggest that cells can generate a continuum of elementary signals, the possibility of predominant amplitudes resulting from the recruitment of preferential subclusters cannot be excluded. This may explain previous observations of apparently stereotypic Ca^{2+} puffs (Yao et al., 1995; Bootman et al., 1997). In support of this, growth in the magnitude of elementary events was observed in a minority of cells (5%, $n = 700$ cells).

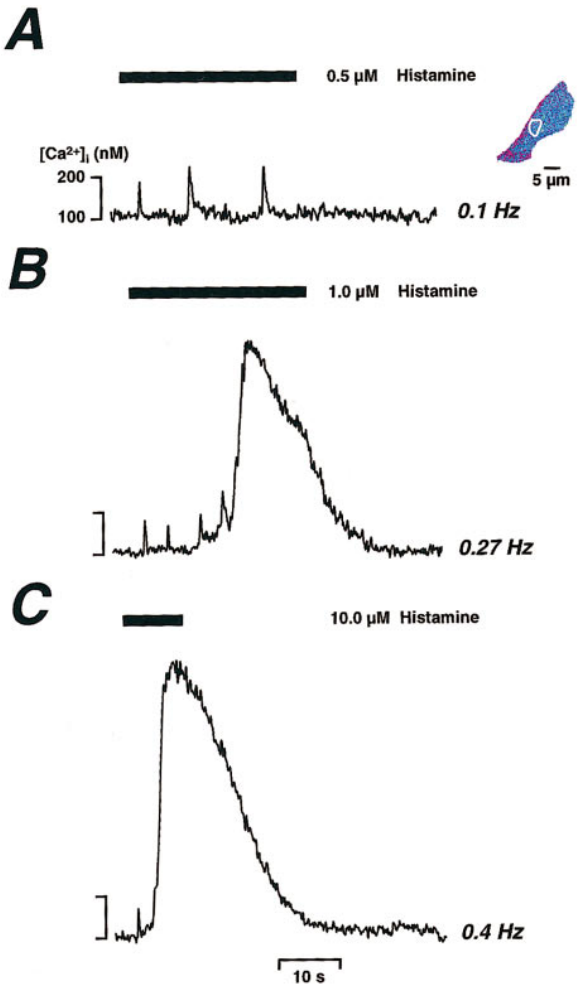

Figure 2. Concentration-Dependent Patterns of Ca^{2+} Release in HeLa Cells

Transition from a nonregenerative response (A) to a regenerative response with a long (B) and brief (C) pacemaker, by increasing histamine concentration. (A–C) represent $[Ca^{2+}]_i$ in the same subcellular location (white area in inset to [A]). (A) Application of 0.5 μM histamine evoked a series of spatially confined, that is, nonregenerative, elementary Ca^{2+} release events, with an average frequency of ~0.1 Hz. (B) Increasing the histamine concentration to 1 μM elevated the frequency of the events to ~0.3 Hz and eventually triggered a propagating Ca^{2+} wave. (C) Further increasing the hormone concentration (10 μM) significantly reduced the duration of the pacemaker phase and raised the frequency to ~0.4 Hz. For each panel, the bar indicates the duration of histamine application. The frequency of the release events was calculated as the reciprocal of the average period between events. For (C), the frequency was taken as the time between the first release event and the inflexion in the upstroke phase of the global Ca^{2+} signal. The cell analyzed in this figure displayed only a single elementary Ca^{2+} release site.

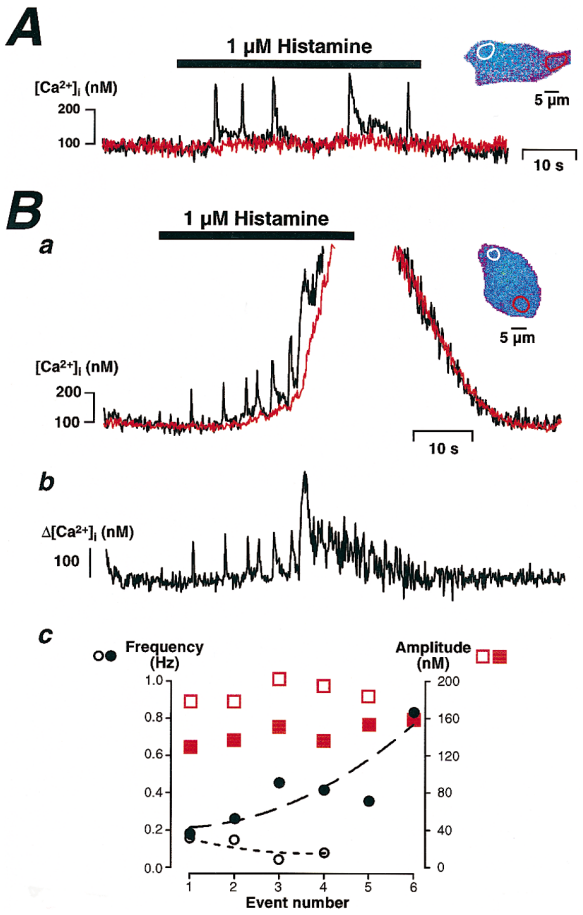

Figure 3. Recruitment of Elementary Ca^{2+} Release Events in the Frequency Domain

Threshold stimulation evoked either nonregenerative Ca^{2+} release events (A) or regenerative Ca^{2+} waves (Ba). The regions with white borders in the cell images in (A), and (Ba) show the sites of elementary Ca^{2+} release. The corresponding $[Ca^{2+}]_i$ signals are plotted in black. To illustrate the "background" change during the pacemaker, $[Ca^{2+}]_i$ in areas shown with red borders are also plotted (red lines). The signals arising from the release events were isolated from the background signal by subtracting $[Ca^{2+}]_i$ in the red line plot from that shown in black. The resulting $\Delta[Ca^{2+}]_i$ trace is plotted in (Bb). (Bc) summarizes the frequency and amplitude characteristics of the elementary events shown (A) and (Ba). The open symbols represent values calculated from the response shown in (A) while closed symbols were obtained from that shown in (B). The frequency of the release events was calculated as the reciprocal of the period between successive events.

Since Ca^{2+} waves propagate throughout HeLa cells by alternating between regeneration at Ca^{2+} release sites and Ca^{2+} diffusion between the release sites, that is, saltatoric Ca^{2+} wave (Bootman et al., 1997), it can be assumed that functional Ca^{2+} releasing units are widely distributed. However, these units are clearly not uniform in their function, as only a few cellular regions exhibit elementary signals during the pacemaker phase. In fact, in the majority of cells (>60%, n = 700) only a single such site was active. Assuming that a representative HeLa cell has a diameter of 30 μm and a thickness of 3 and 10 μm in the periphery and nuclear regions, respectively (unpublished data), the volume occupied by a single Ca^{2+} puff is <3% that of the total cellular volume. This indicates that Ca^{2+} signals occupying a fraction of the cellular volume are capable of driving the cell to threshold. The upper limit of elementary release sites that were observed to be contributing to pacemaking was six. The reason that cells utilize a variable number of release sites during the pacemaker phase is unclear. There was no obvious correlation between cell size or dimension and the number of sites. In addition, repeated stimulation of the cells always recruited the

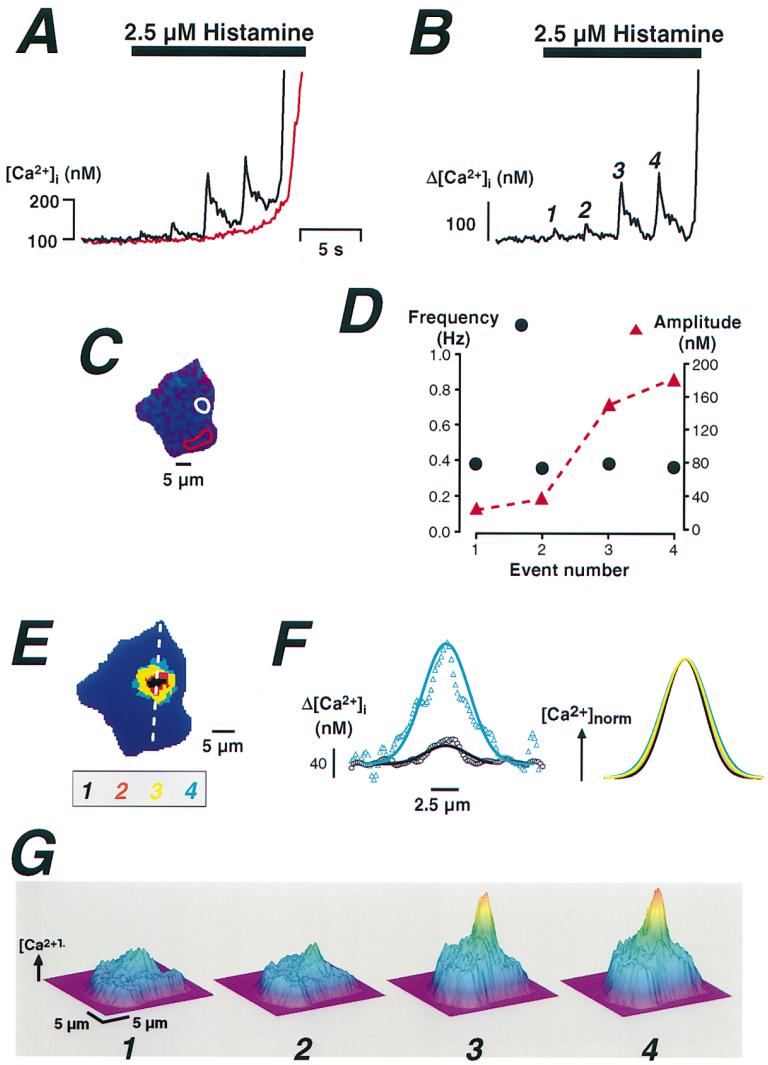

Figure 4. Recruitment of Elementary Ca^{2+} Release Events in the Amplitude Domain

A regenerative Ca^{2+} wave (A) was triggered by four elementary release events that displayed a constant frequency (closed circles in [D]) but a 9-fold increase in amplitude. The region with white borders in the cell image in (C) shows the site of elementary Ca^{2+} release. (A) shows the corresponding $[Ca^{2+}]_i$ signals plotted in black. The background $[Ca^{2+}]_i$ change during the pacemaker (taken from the cell area in [C] with red border) is shown by the red line in (A). The $\Delta[Ca^{2+}]_i$ (B) arising from the release events was obtained by subtracting $[Ca^{2+}]_i$ in the red line plot from that shown in black. The amplitudes and frequencies of the release events are shown in (D). The frequency was calculated as the reciprocal of the period between successive events. For simplicity, only the pacemaker phase is shown. (E) The elementary release events arose from the same locus. The subcellular location of the release events was visualized from images at peak amplitude, which were thresholded at a level corresponding to 50% of the peak $[Ca^{2+}]_i$ signal. Areas above the 50% threshold were color coded according to the scheme shown in (E) and stacked on top of a cell image at rest. (F) shows an analysis of the $[Ca^{2+}]_i$ distribution at the peak of the four signals. Curves were fitted to the spatial spread of the signal, assuming a Gaussian distribution of $[Ca^{2+}]_i$. The left panel in (F) shows the fit for the smallest (1, black) and largest (4, light blue) events. After superposition of the normalized curves, the distributions were found to coincide, indicating a common Ca^{2+} point source. (G) illustrates the spatial properties of the four individual Ca^{2+} release events as surface representations. $[Ca^{2+}]_i$ is coded in both the height and color of the surface.

same elementary release sites (e.g., Figure 2). These observations suggest that the elementary release sites active during the pacemaker phase were distinct from those simply aiding Ca^{2+} wave propagation (e.g., they possessed a higher sensitivity to stimulation). This indicates that recruitment of Ca^{2+} release events in HeLa cells is not a spatially probabilistic phenomenon, like Ca^{2+} sparks in excitable cells. Instead, HeLa cells displayed "eager" Ca^{2+} release sites operating during pacemaking.

Recruitment in the Spatial Domain

The spatio-temporal properties of pacemaker responses with multiple elementary sites were more complex than those with only a single site. However, the same principles of frequency and/or amplitude recruitment accounted for regenerative responses in these cells. An example showing the recruitment of multiple release sites is illustrated in Figure 5. This cell displayed five distinct release sites along the line scanned. One site (trace 4 in Figure 5B) was eager during the pacemaker phase, since it displayed a higher release frequency than the other identified sites. However, the signals from this region did not alter in frequency or amplitude, suggesting that it would not by itself cause regenerativity. As the pacemaker phase proceeded, additional elementary release units were recruited from neighboring regions, resulting in a gradual increase of the cumulative release frequency (Figure 5C).

Synergism between Frequency, Amplitude, and Spatial Domains

Although pacemaking advances in either frequency, amplitude, or spatial domains, not all attempts to achieve regenerativity were equally successful. In cases such as that shown in Figure 6, the synergistic interplay between all three domains was necessary. This cell displayed two successive pacemaker phases (graded bars in Figure 6B), despite continuous agonist stimulation. Pacemaker phase 1 resulted in an abortive response, while pacemaker phase 2 evoked a propagating Ca^{2+} wave. Presumably a change in the balance between the positive and negative feedback mechanisms caused the first pacemaker to fail, but the frequency, amplitude, and spatial recruitment of Ca^{2+} release sites advanced

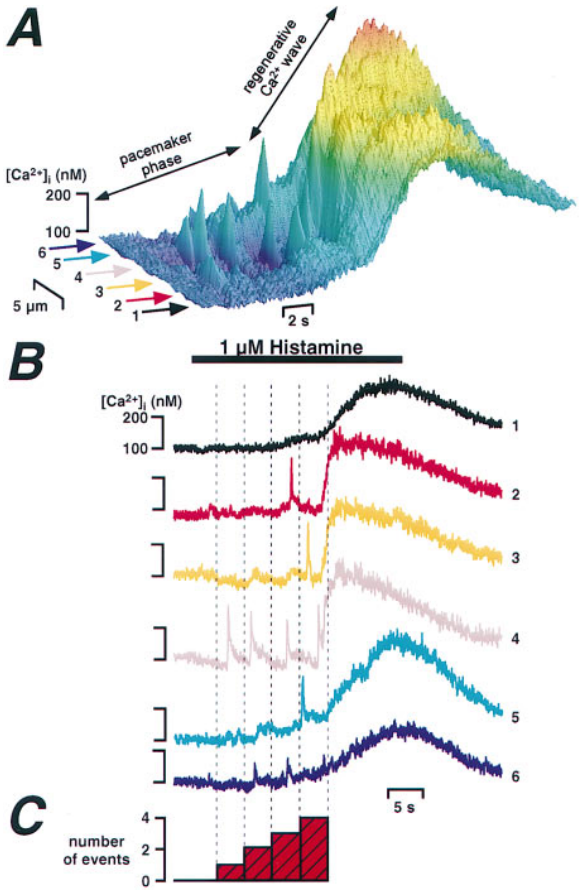

Figure 5. Recruitment of Elementary Ca^{2+} Release Events in the Spatial Domain

(A) Surface representation of a line scan (4 ms per line) obtained during threshold stimulation displaying five different elementary Ca^{2+} release sites. $[Ca^{2+}]_i$ is coded in both the height and the color of the surface. The $[Ca^{2+}]_i$ at these release sites (lower 5 traces in [B]) and at one remote site (black trace in [B]) was calculated by averaging the signal in 2 µm wide bands along the lines centered around the arrowheads in (A). The colors and the labeling of the arrowheads in (A) correspond to the line plots in (B). (C) shows the increasing cumulative frequency of elementary signals, derived by counting the events occurring in 4 s–long segments.

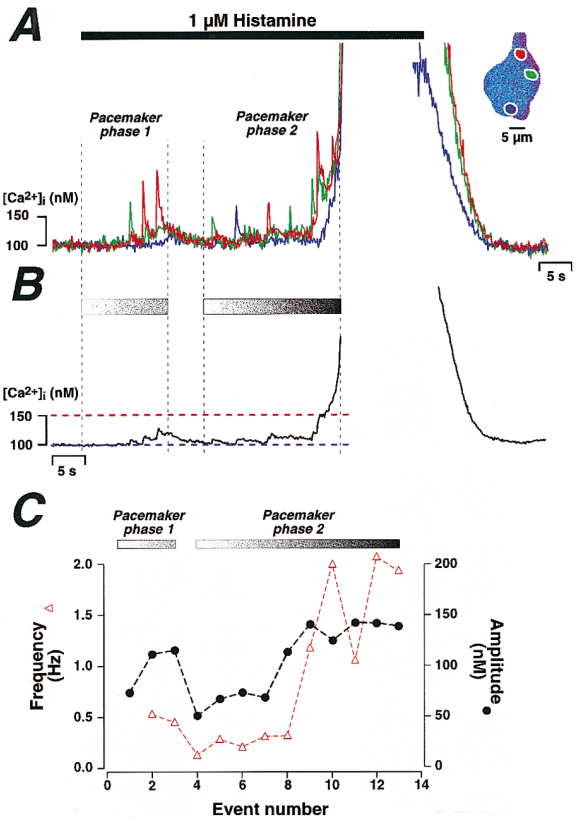

Figure 6. Synergism between Frequency, Amplitude, and Spatial Domains

(A) $[Ca^{2+}]_i$ traces derived from three different elementary release sites. The subcellular locations of the release sites are marked on the cell image with corresponding colors. The overall pacemaker activity was considered to comprise two individual pacemaker phases. These phases are denoted by the two pairs of vertical dotted lines as pacemaker phase 1 and pacemaker phase 2. During pacemaker phase 1, there was a transient burst of release activity resulting from recruitment in all three domains. During pacemaker phase 2, the activity recovered and, following advances in the three domains, eventually triggered a Ca^{2+} wave.

(B) The effect of the pacemaker activity on global $[Ca^{2+}]_i$ (averaged over the entire confocal section). The plot suggests that during pacemaker phase 1, global $[Ca^{2+}]_i$ did not reach the threshold level (red dotted line), but the Ca^{2+} release activity in pacemaker phase 2 was sufficient. The dotted blue line marks resting $[Ca^{2+}]_i$.

(C) The frequencies and the amplitudes of the elementary Ca^{2+} release events from pacemaker phase 1 and 2 are plotted.

sufficiently during the second phase to trigger regenerativity.

The failure of pacemaker phase 1 provides important evidence as to the nature of the threshold for regenerativity. Although we have demonstrated that in those cells which become regenerative, the pacemaker activity always progressed at least in one of the three domains, we suggest that elementary events themselves are not the direct cause for regenerativity. It appears that the elementary events during pacemaking drive the ambient $[Ca^{2+}]_i$ toward the threshold (Figure 6B). The integration of the elementary Ca^{2+} signals by the cytoplasm links the frequency, amplitude, and spatial domains to the global mechanisms responsible for regenerativity. It is therefore obvious why the first pacemaking activity failed; the global $[Ca^{2+}]_i$ did not reach the critical level. Studies using excitable cells have similarly suggested a critical Ca^{2+} threshold for regenerativity (Friel and Tsien, 1992; Iino et al., 1993).

Despite revealing that regenerativity occurs by advancing elementary events in the three domains to give a threshold $[Ca^{2+}]_i$, two fundamental questions remain: 1) what happens locally to advance the elementary signals, and 2) what happens globally to evoke regenerativity when threshold is reached? The answers to these questions are complex since Ca^{2+} can have a multiplicity of effects, involving processes that contribute additional positive or negative feedback to local and global Ca^{2+} release. For the elementary signals, the most prominent effects are probably on the release units themselves. Spatially restricted Ca^{2+} release from $InsP_3Rs$ can be

modulated by [$InsP_3$] and the well-known bimodal effect of Ca^{2+} on $InsP_3R$ (Bezprozvanny and Ehrlich, 1995). The precise balance between local negative and positive feedback determines whether elementary signals will advance or decline in any of the three domains. In addition, local events will be influenced by the global contribution of remote signals.

The development of regenerativity is critically dependent on the integrating ability of the cytoplasmic compartment. Essentially, the whole mechanism can be simplified to the fine balance between Ca^{2+} release and removal. The key processes modulating Ca^{2+} release are Ca^{2+}-dependent feedback on $InsP_3Rs$ (Bezprozvanny et al., 1991; Iino and Endo, 1992; Missiaen et al., 1994; Bootman et al., 1995) and phospholipase C (Wojcikiewicz and Nahorski, 1993; Bootman et al., 1996). These positive feedback loops serve to further enhance elementary activity and hence feed cytoplasmic Ca^{2+}. Conversely, the integrated Ca^{2+} signal will also activate negative feedback components, such as protein kinase C and Ca^{2+} pumps (Petersen et al., 1994). These serve to diminish elementary activity. The balance between these mechanisms determines whether a cell will become regenerative. From this, it follows that the threshold represents the virtual point at which the effects of positive and negative feedback are equalized.

We believe that the domains of frequency, amplitude, and spatial recruitment identified here are general principles underlying Ca^{2+} signaling in nonexcitable cells. Ca^{2+} signal transduction in such cells comprises a series of transitions between analog and digital signals. The analog hormone signal is converted into digital elementary Ca^{2+} release signals, which are integrated into an analog $[Ca^{2+}]_i$ transient, and above the threshold this evokes global oscillations. A series of such digital oscillations is eventually converted into an analog response from the cell (e.g., cell growth). Due to this multimode transduction cascade, nonexcitable cells can fine-tune spatial and temporal aspects of their responses.

Experimental Procedures

Cell Culture

HeLa cells were grown on 40 mm glass coverslips as described elsewhere (Bootman et al., 1997). Prior to the experiments, coverslips were mounted in a sandwich chamber, and the cells were loaded with 3 μM Fluo-3AM (Molecular Probes, Eugene, OR) for 30 min at room temperature (20°C–22°C). Thereafter, the Fluo-3AM was washed off and exchanged with an extracellular solution containing (in mM): NaCl 121, KCl 5.4, $MgCl_2$ 0.8, $CaCl_2$ 1.8, $NaHCO_3$ 6, glucose 5.5, HEPES 25 adjusted to pH 7.3 with NaOH. The cells were allowed to deesterify for an additional 30 min. Histamine was applied ($\tau_{1/2}$ of solution exchange $<$500 ms) by means of a homemade solenoid-driven rapid switching device. All experiments were carried out at 20°C–22°C.

Ca^{2+} Measurements

Confocal imaging of the Fluo-3 loaded HeLa cells was performed with NORAN Odyssey and Oz confocal microscopes (NORAN Instruments, Milton Keynes, UK). The slit apertures of the instruments were adjusted to give a confocal z-section depth of ~1.5 μm. Confocal recordings were performed either as a time series of confocal images (240 × 320 pixels, at 7.5–15 Hz) or by repetitive scanning (250 Hz) of a single line from the confocal section. Data analysis and processing were performed as described previously (Bootman et al., 1997).

Acknowledgments

M. D. B. gratefully acknowledges the support of a Royal Society University Research Fellow.

Received August 7, 1997; revised September 16, 1997.

References

Berridge, M.J. (1993). Inositol trisphosphate and calcium signaling. Nature *361*, 315–325.

Berridge, M.J. (1997). Elementary and global aspects of calcium signaling. J. Physiol. *499*, 291

Bezprozvanny, I., and Ehrlich, B.E. (1995). The inositol 1,4,5-trisphosphate ($InsP_3$) receptor. J. Membr. Biol. *145*, 205–216.

Bezprozvanny, I., Watras, J., and Ehrlich, B.E. (1991). Bell-shaped calcium response curves of Ins(1,4,5)P_3-gated and calcium-gated channels form endoplasmic reticulum of cerebellum. Nature *351*, 751–754.

Bootman, M.D. (1996). Hormone-evoked subcellular Ca^{2+} signals in HeLa cells. Cell Calcium *20*, 97–104.

Bootman, M.D., and Berridge, M.J. (1995). The elemental principles of calcium signaling. Cell *83*, 675–678.

Bootman, M.D., Taylor, C.W., and Berridge, M.J. (1992). The thiol reagent, thimerosal, evokes Ca^{2+} spikes by sensitizing the inositol 1,4,5-trisphosphate receptor. J. Biol. Chem. *267*, 25113–25119.

Bootman, M.D., Missiaen, L., Parys, J.B., De Smedt, H., and Casteels, R. (1995). Control of inositol 1,4,5-trisphosphate-induced Ca^{2+} release by cytosolic Ca^{2+}. Biochem. J. *306*, 445–451.

Bootman, M.D., Young, K.W., Young, J.M., Moreton, R.B., and Berridge, M.J. (1996). Extracellular calcium concentration controls the frequency of intracellular calcium spiking independently of inositol 1,4,5-trisphosphate production in HeLa cells. Biochem. J. *314*, 347–354.

Bootman, M.D., Niggli, E., Berridge, M.J., and Lipp, P. (1997). Imaging the hierarchical Ca^{2+} signaling system in HeLa cells. J. Physiol. *499*, 307–314.

Cheng, H., Lederer, W.J., and Cannell, M.B. (1993). Calcium sparks—elementary events underlying excitation–contraction coupling in heart muscle. Science *262*, 740–744.

Clapham, D.E. (1995). Calcium signaling. Cell *80,* 259–268.

Friel, D.D., and Tsien, R.W. (1992). Phase-dependent contributions of Ca^{2+} entry and Ca^{2+} release to caffeine-induced $[Ca^{2+}]_i$ oscillations in bullfrog sympathetic neurons. Neuron *8*, 1109–1125.

Iino, M., and Endo, M. (1992). Calcium-dependent immediate feedback-control of inositol 1,4,5-trisphosphate–induced Ca^{2+} release. Nature *360*, 76–78.

Iino, M., Yamazawa, T., Miyashita, Y., Endo, M., and Kasai, H. (1993). Critical intracellular calcium concentration for all-or-none spiking in single smooth muscle cells. EMBO J. *12*, 5287–5291.

Lechleiter, J., Girard, S., Clapham, D., and Peralta, E. (1991). Subcellular patterns of calcium release determined by G protein-specific residues of muscarinic receptors. Nature *350*, 505–508.

Lipp, P., and Niggli, E. (1994). Modulation of Ca^{2+} release in cultured neonatal rat cardiac myocytes—insight from subcellular release patterns revealed by confocal microscopy. Circ. Res. *74*, 979–990.

Lipp, P., and Niggli, E. (1996). A hierarchical concept of cellular and subcellular Ca^{2+} signaling. Prog. Biophys. Mol. Biol. *65*, 265–296.

Lipp, P., and Bootman, M.D. (1997). To quark or to spark, that is the question. J. Physiol. *502*, 1–2.

López-López, J.R., Shacklock, P.S., Balke, C.W., and Wier, W.G. (1995). Local calcium transients triggered by single L-type calcium channel currents in cardiac cells. Science *268*, 1042–1045.

Missiaen, L., Parys, J.B., De Smedt, H., and Casteels, R. (1994). Coactivation of inositol trisphosphate-induced Ca^{2+} release by cytosolic Ca^{2+} is loading dependent. J. Biol. Chem. *269*, 7238–7242.

Parker, I., and Yao, Y. (1991). Regenerative release of calcium from

functionally discrete subcellular stores by inositol trisphosphate. Proc. R. Soc. Lond. *246*, 269–274.

Parker, I., and Yao, Y. (1996). Ca^{2+} transients associated with openings of inositol trisphosphate-gated channels in Xenopus oocytes. J. Physiol. *491*, 663–668.

Petersen, O.H., Petersen, C.C.H., and Kasai, H. (1994). Calcium and hormone action. Annu. Rev. Physiol. *56*, 297–319.

Reber, B.F.X., and Schindleholz, A. (1996). Detection of a trigger zone of bradykinin-induced fast calcium waves in PC12 neurites. Pflügers Arch. *432*, 893–903.

Thomas, A.P., Renard, D.C., and Rooney, T.A. (1991). Spatial and temporal organization of calcium signaling in hepatocytes. Cell Calcium *12*, 111–126.

Wojcikiewicz, R.J.H., and Nahorski, S.R. (1993). Modulation of calcium signaling initiated by phosphoinositidase-linked receptors. J. Exp. Biol. *184*, 145–159.

Yao, Y., Choi, J., and Parker, I. (1995). Quantal puffs of intracellular Ca^{2+} evoked by inositol trisphosphate in Xenopus oocytes. J. Physiol. *482*, 533–553.